ELSEVIER

Journal of Crystal Growth 163 (1996) 113–121

JOURNAL OF CRYSTAL GROWTH

Predicted structures and stabilities of the surface A grooves and double bilayer height steps on the GaAs(001)-2 × 4 surface

S.B. Zhang *, Alex Zunger

National Renewable Energy Laboratory, Golden, Colorado 80401, USA

Abstract

"A-type" surface steps on GaAs(001) have edges parallel to the direction of the As–As dimers. We identify here two series of A step structures on this surface: the "groove structures" and the "double bilayer height steps". Both can be thought as being obtained by cleaving the flat 2 × 4 surfaces into two bilayer height step segments and reassembling these segments into step structures. The relative stabilities of these two step structures and their stabilities with respect to other low energy A step structures are examined using our newly developed method of "linear combination of structural motifs". We find that (i) for a given separation S (in units of surface atomic spacing a_s) between the two step segments the grooves are more stable than the double bilayer steps; (ii) the $S = 1$ A groove is predicted to be the most stable A groove structure, whereas (iii) the $S = 0$ double A step is predicted to be the most stable A step structure over a wide range of the Ga chemical potential.

1. Introduction

The nominally flat GaAs(001) surface exhibits a range of reconstruction patterns depending on the anion-to-cation ratio. Recent STM experiments [1–6] and calculations [7,8] have shown that the anion rich $\beta 2(2 \times 4)$ reconstruction is stable over a wide range of atomic chemical potentials. This reconstruction (Fig. 1a) involves the formation of As–As dimers: the top surface layer has two missing dimers for each four dimers in a row. A third As–As dimer is present in the second subsurface layer, inside the trough left by the missing dimers in the top layer. Despite the fact that reconstructed, nominally flat surfaces represent the *lowest energy* surface configurations as revealed by surface annealing experiments [9], surface steps tend to form during growth. There are two commonly observed [9–11] steps on GaAs(001) those with step edges parallel to the direction of the As–As dimers ("A steps") and those with step edges perpendicular to the dimer direction ("B steps"). One can envision a large number of atomic models for these steps. Some of the simple models have been discussed in Ref. [12]. We showed [12] that while the formation of both A and B steps from a nominally flat GaAs(001)-$\beta 2(2 \times 4)$ surface requires an *investment* of energy (i.e., the formation energies are positive), the formation energies of the simple model A steps are lower than those of B steps. We report here on two types of A steps that are predicted to have particularly low formation energies. Both can be described starting from the atomic structure of the $\beta 2(2 \times 4)$ reconstruction by noting that this surface contains an atomic trough within each unit cell (see Fig. 1a). "Cleaving" this structure along "cleavage

* Corresponding author.

0022-0248/96/$15.00 © 1996 Elsevier Science B.V. All rights reserved
SSDI 0022-0248(95)01053-X

line 1" inside the trough (dashed line in Fig. 1a) leads to a primitive AI(r) and a primitive AII(l) step (Fig. 1b) where the indices r and l indicate the right and left step orientations, respectively. One can alternatively form the mirror images of these steps (denoted here by AI(l) and AII(r) steps, see Fig. 1c) by cleaving at the "cleavage line 2". These "primitive steps" lead naturally to two different series of step structures on GaAs(001)-$\beta 2(2\times4)$ surfaces:

(i) *The AI + AII (S) grooves*: This series of groove structures is formed by inserting S units of "flat" $\beta 2(2\times4)$ surface unit cells between the AI(r) and AII(l) primitive steps (see Fig. 1b). The inserted flat surface segments are lower by one bilayer height unit relative to the starting surface. The resulting structure is a bilayer height groove with two steps and a net zero height variation in going across the groove. We illustrate in Fig. 2a the $S=1$ groove. Note that in the limit of $S=0$, one recovers from the AI + AII (S) grooves the ordinary $\beta 2(2\times4)$ surface. Grooves represent an important part of the realistic stepped surfaces.

(ii) *The double (bilayer height) A (S) steps*: One can also combine the AI(r) step of Fig. 1b with an AII(r) step of Fig. 1c. This leads to the "$S=0$ double bilayer height A step" shown in Fig. 2b. Note that different from the A grooves, here the AI(r) + AII(r) combination (not shown) has a slightly higher energy than the AII(r) + AI(r) combination (shown in Fig. 2b). In analogy with the AI + AII (S) grooves, here too one can insert between the AI and AII segments S units of the "flat" $\beta 2(2\times4)$ surface unit cells. In contrast to the AI + AII (S) grooves, however, the net height variation across the double A steps is two, instead of zero, bilayers. Thus, this structure does not become a $\beta 2(2\times4)$ structure at $S=0$.

In this work, we calculate the formation energies of the AI + AII grooves and the double A steps as a function of S. We find that while the formation energy increases monotonically with S, at a fixed S the AI + AII groove is more stable than the corresponding double A step. Comparing to other candidate groove and single step structures, our calculation shows that over a large range of the Ga chemical potential, μ_{Ga} the $S=1$ AI + AII groove is the most stable "A groove structure" whereas the $S=0$ double A step is the most stable "A step structure".

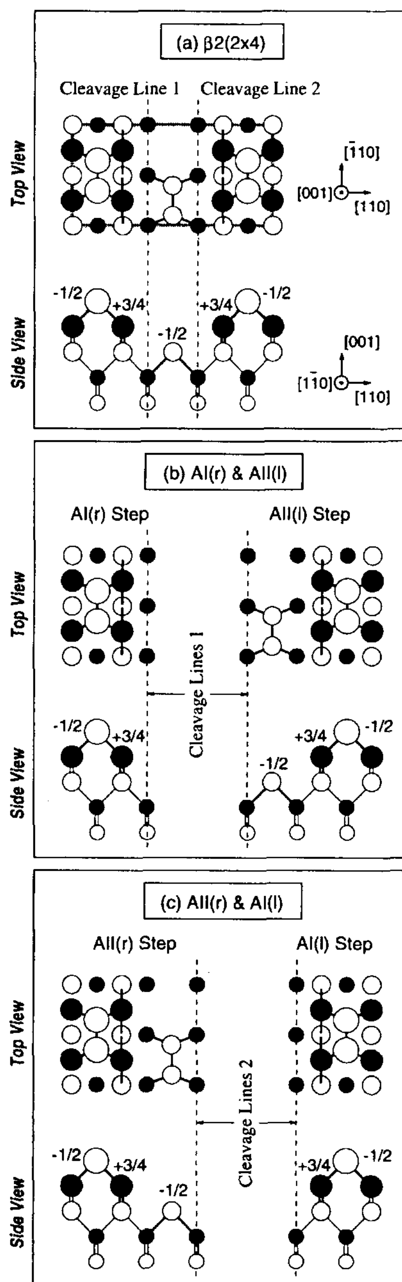

Fig. 1. Top and side views of (a) a $\beta 2(2\times4)$ surface unit cell, (b) the AI(r) AII(l) step pair, and (c) the AII(r) and AI(l) step pair. The open and filled circles are As and Ga atoms, respectively. In progressing from the top surface into the surface interior, the sizes of these atoms decrease. The numbers indicated in the side views show the charge Q for surface atoms. The thicker bond lines indicate surface bonds shown in the top view.

2. Method

In a previous paper [13] we have described the method of "linear combination of structural motifs" (LCSM) for calculating surface and surface step formation energies. Here, we give a brief description of the method, as applied to A steps on GaAs(001).

The method is based on two observations distilled from previous ab initio geometry optimizations on flat GaAs(001) surfaces [14] and on bulk point defects [15]. *First*, a relatively large collection of calculated surface structures and bulk point defects can be built from a limited number of recurring local "structural motifs", including (in GaAs) tetrahedrally bonded Ga and As, threefold coordinated pyramidal As, threefold coordinated planar Ga, and twofold coordinated bridge site Ga. *Second*, the atomic structure that corresponds to a stable surface

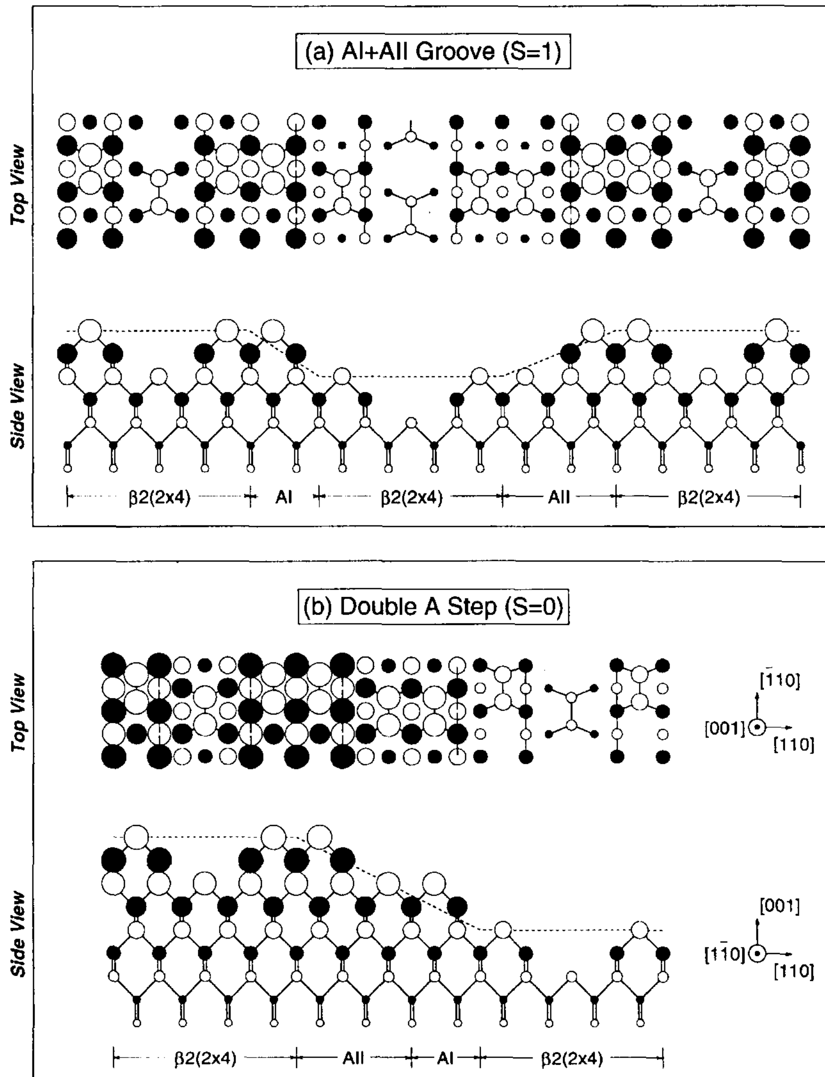

Fig. 2. Top and side views of (a) the $S = 1$ AI + AII groove and (b) the $S = 0$ double A step. The dashed lines show profiles of the stepped surfaces when the atomic troughs of the "flat" $\beta2(2\times4)$ surfaces are ignored. The open and filled circles are As and Ga atoms, respectively, with decreasing sizes from surface into bulk.

is such that (i) the surface band gap levels are emptied and (ii) oppositely charged, miscoordinated atomic sites charge-compensate each other. In the simplest cases, these atomic sites form charge compensated "donor–acceptor" pairs. As results, the total energy of a system (or a structure) σ (= bulk point defects, surfaces or steps) can be written as

$$E(\sigma,\mu_R) = E_{LCSM}(\sigma) + E_{Mad}(\sigma) + E_R(\sigma,\mu_R), \quad (1)$$

where

$$E_{LCSM}(\sigma) = \sum_M \omega_M(\sigma)\epsilon_M \quad (2)$$

is a linear combination of structural motif energies ϵ_M with $\omega_M(\sigma)$ being the frequency of occurrence of motif M in the structure σ. We use the same characteristic motif energy ϵ_M for motif M, irrespective of the identity of its neighbors. The effects of different nearest neighbor atoms are implemented through two-site "wrong bond" motifs and by the long range interactions described electrostatically by a Madelung energy,

$$E_{Mad}(\sigma) = \frac{1}{2\epsilon}\sum_{ij}{}' \frac{Q_i Q_j}{|R_i - R_j|}. \quad (3)$$

Here, Q_i is the charge of the ith atom at position R_i resulting from adherence to the octet rule [13], and ϵ is the effective dielectric constant. The last term in Eq. (1) is the "reservoir energy"

$$E_R(\sigma,\mu_R) = \Sigma\mu_R N_R. \quad (4)$$

We assume that the system σ is in equilibrium with a reservoir R, containing N_{Ga} of free Ga atoms and N_{As} of free As atoms with chemical potentials μ_{Ga} and μ_{As}, and N_e of free electrons with a Fermi energy μ_e. The term of Eq. (4) is needed in order to account for both material and electron balance in a chemical reaction from a reference system σ_0 to system σ, $\sigma_0 \to \sigma$.

For surfaces and surface steps, the formation energy of the system σ relative to σ_0 is

$$\Delta E(\sigma,\mu_R) \equiv E(\sigma,\mu_R) - E(\sigma_0,\mu_R) = \Delta E_{LCSM}(\sigma) + \Delta E_{Mad}(\sigma) + \Delta E_R(\sigma,\mu_R), \quad (5)$$

where each term is a difference with respect to σ_0. Here, $\Delta E(\sigma,\mu_R)$ is only a function of the atomic chemical potential, μ_{Ga} and μ_{As}, and not a function of the electron chemical potential, μ_e, due to surface charge compensation, $\Delta N_e \equiv 0$. In addition, under thermal equilibrium between surface and bulk GaAs, the chemical potentials of Ga and As satisfy

$$\mu_{Ga} + \mu_{As} = -\Delta H, \quad (6)$$

where $\Delta H = 0.92$ eV is the calculated heat of formation of GaAs [7]. Eq. (6) allows us to express the formation energy $\Delta E(\sigma,\mu_R)$ as a function of the Ga chemical potential, μ_{Ga} alone. Note that the limit $\mu_{Ga} = 0$ corresponds to the Ga-rich limit. The more negative is μ_{Ga}, the more "As-rich" or "Ga-poor" is the surface. The As-rich limit can be reached when $\mu_{Ga} = -\Delta H = -0.92$ eV.

For each surface, or step structure σ we know $\{\omega_M\}$ (by counting motifs), as well as $\{N_R\}$ (by counting atoms and electrons) and the charge $\{Q_i\}$ (by applying the octet rule). The unknowns are the surface dielectric constant ϵ_s and the motif energies $\{\epsilon_M\}$. These were obtained in Ref. [13] by fitting Eq. (1) to a set of pseudopotential local density approximation (LDA) calculations on bulk point defects and on nominally flat GaAs(001) surfaces. The pseudopotential calculations on surfaces involve relaxing all atoms coordinates to zero-force positions. At these equilibrium geometry, not all bond lengths and angles have the ideal bulk value, so in this sense the surface is atomically strained. Since the pseudopotential total energies pertain to strained surfaces, the motif energies extracted from the pseudopotential energies do include strain effects. However, any *long range* macroscopic strain effects associated with the steps are precluded. The reliability of the LCSM approach was tested by its ability to reproduce the energies of *independently calculated* LDA surface structures (see below) and surface steps (detailed in Ref. [13]).

Fig. 3 shows the dependence of the surface formation energies on Ga chemical potential as obtained by first-principles calculations (Part a) and by the LCSM method (Part b). The stoichiometric $\alpha(2\times4)$ surface is used here as a reference. From Eqs. (1) and (4), surface formation energy is a linear function of μ_{Ga}. Positive slopes indicate As-rich surfaces whereas negative slopes indicate Ga-rich surfaces.

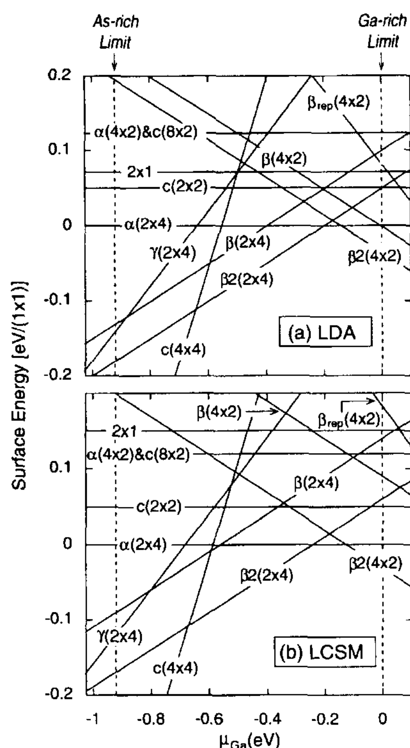

Fig. 3. GaAs(001) surface formation energies in units of (1×1) surface area are shown as a function of the Ga chemical potential: (a) LDA results from Refs. [7,14] and (b) the LCSM results from Ref. [13]. The energy of the $\alpha(2 \times 4)$ surface is used here as reference. The range of the Ga chemical potential is indicated here by two vertical dashed lines at which either solid As or solid Ga will start to deposit on the surface, thus prohibiting any further change in μ_{Ga}.

Taking the $\beta 2(2 \times 4)$ structure as an example, it is unstable for excessive As-rich surfaces, i.e., $\mu_{Ga} < -0.64$ eV. For $-0.64 \text{ eV} < \mu_{Ga} < -0.2$ eV, the $\beta 2(2 \times 4)$ structure is stable. At $\mu_{Ga} = -0.2$ eV, transition from $\beta 2(2 \times 4)$ to $\alpha(2 \times 4)$ takes place. Only the energies of the $\beta 2(4 \times 2)$, $c(8 \times 2)$ and $c(2 \times 2)$ surfaces were fitted in the LCSM calculations whereas all others are predicted with an overall accuracy of ± 0.05 eV per surface atom.

Once the parameters were obtained, Eq. (1) allows us to evaluate the formation energy of complicated surface and surface step structures, as detailed in Refs. [13,16]. The flat $\beta 2(2 \times 4)$ surface (Fig. 1a), the AI + AII grooves (Fig. 2a), and the double A steps (Fig. 2b) represent a special set of structures on the surface having identical surface motifs {M} and identical motifs frequencies $\{\omega_M\}$ (i.e., chemically identical). As a consequence, in constructing the AI + AII grooves and the double A steps from the $\beta 2(2 \times 4)$ surface, we do not need to transfer any atom between the surfaces and atomic reservoirs. In other words, the formation energies of the AI + AII grooves and the double A steps from the parent $\beta 2(2 \times 4)$ flat surface are independent of the atomic chemical potential, μ_{Ga}. The only term in Eq. (1) responsible for the energy differences among this set of structures is thus the Madelung term ΔE_{Mad} for which the numerical uncertainty is exceedingly small. Note, however, that other step structures considered in Section 3.2 have contributions from all terms of Eq. (1). The uncertainty here is estimated to be ± 0.03 eV per unit $(1 \times)$ bilayer step.

In the following, we will discuss, as an example, how the point charges Q_i which enter the calculation of ΔE_{Mad} for the $\beta 2(2 \times 4)$ surface, the AI + AII grooves, and the double A steps are derived using the octet rule. There exist four different types of motifs on these surfaces: denoting coordination number by superscripts, these include fourfold coordinated bulk $Ga^{(4)}$ and $As^{(4)}$ atoms, and threefold coordinated surface $Ga^{(3)}$ and $As^{(3)}$ atoms. Note that a $Ga^{(4)}$ atom has four bonds, 3 valence electrons and a nuclear charge of 3 +. The octet rule states that the $Ga^{(4)}$ atom contributes 3/4 electron to each of its four bonds, thereby maintaining a *local* charge neutrality. Similarly, a fourfold coordinated $As^{(4)}$ atom has 5 valence electrons and a nuclear charge of 5 +; the $As^{(4)}$ atom thus contributes 5/4 electrons to its four bonds becoming also locally neutral, i.e.

$$Ga^{(4)} \to Q = 0$$

$$As^{(4)} \to Q = 0. \quad (7)$$

In calculating the charges on the surface atoms, we maintain the above bulk "partition rule". Thus a surface $Ga^{(3)}$ atom, with three bulk $As^{(4)}$ nearest neighbors, contributes a total of $3 \times 3/4$ electrons to the three bulk Ga–As bonds, leaving behind $3 - 3 \times 3/4 = 3/4$ electron in the fourth (dangling) bond. In contrast, a surface $As^{(3)}$ atom, with two bulk $Ga^{(4)}$ and one surface $As^{(3)}$ nearest neighbors, contributes a total of $2 \times 5/4 + 1 = 7/2$ electrons to the two bulk Ga–As bonds and the one surface As–As bond. Here, we assume that the two As atoms in an As–As

dimer are indistinguishable, thus each contributes one electron to the dimer bond. This leaves behind $5 - 7/2 = 3/2$ electrons in the As dangling bond. It is well known [8] that the $Ga^{(3)}$ dangling bond orbital is located near the bulk conduction band minimum, whereas the $As^{(3)}$ dangling bond orbital is located near the bulk valence band maximum. Here, the octet rule states that by donating 3/4 electron, the $Ga^{(3)}$ dangling bond orbital is fully emptied. Conversely, by acquiring 1/2 electron, the $As^{(3)}$ dangling bond orbital becomes completely full. This leads to

$$Ga^{(3)} \to Q = +3/4$$
$$As^{(3)} \to Q = -1/2. \quad (8)$$

The charge assignments for the $\beta2(2\times4)$ surface, and the primitive AI and AII steps are shown in the lower part of Figs. 1a–1c. With these assignments, one can show that the primitive AI and AII steps have a charge density $\eta_{AI} = +\frac{1}{4}/(1\times)$ and $\eta_{AII} = -\frac{1}{4}/(1\times)$, respectively. Here, $(1\times)$ denotes the separation between two nearest neighbor surface atoms of an unrelaxed GaAs(001) surface along the A step edge, $a_s = a/\sqrt{2}$ where a is the GaAs bulk lattice constant. Since $\eta_{AI} + \eta_{AII} \equiv 0$, both the AI + AII grooves and the double A steps are always charge neutral.

3. Results

3.1. Comparison of the AI + AII groove and double A step energies

Fig. 4 shows the formation energy of the AI + AII grooves and the double A steps for $S = 0,1,2$ with respect to the flat $\beta2(2\times4)$ surface. We see from Fig. 4 the following:

(i) *The magnitude of the formation energy:* The formation energies at small S are in the range of < 0.05 eV.

(ii) *Trends in the formation energies:* The formation energy increases monotonically with S. This is because the interaction between the AI and AII steps is *attractive*. To see this, we rewrite Eq. (3) in terms of intra- (i.e., restricting the indices i and j in Eq. (3) to either AI or to AII steps) and inter-step (i.e.,

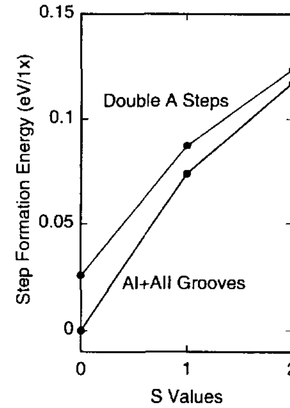

Fig. 4. Step formation energy versus the S parameter for the AI + AII grooves and the double A steps. The reference energy is that of the flat $\beta2(2\times4)$ surface.

restricting the index i in Eq. (3) to an AI step whereas j represents an AII step, and vice versa) interactions. This leads to

$$E_{Mad}(\sigma) = \frac{1}{\epsilon}\left(\sum_{i\in AI}\sum_{j\in AI}{}' \frac{Q_iQ_j}{|R_i - R_j|} + \sum_{i\in AI}\sum_{j\in AII} \frac{Q_iQ_j}{|R_i - R_j|}\right). \quad (9)$$

The first term in Eq. (9) (the intra-step Coulombic interaction) is independent of the step separation parameter S. Thus, only the second term is responsible for the change in Madelung energy, i.e.,

$$\Delta E_{Mad}(\sigma) = \frac{1}{\epsilon}\left(\sum_{i\in AI}\sum_{j\in AII} \frac{Q_iQ_j}{|R_i - R_j|[\sigma]} - \sum_{i\in AI}\sum_{j\in AII} \frac{Q_iQ_j}{|R_i - R_j|[\sigma_0]}\right). \quad (10)$$

In most cases, the separation between the AI and AII steps ($L = 4a_sS$ where $S = 0,1,2,...$) is much larger than the separation between any two adjacent point charges within each of the steps ($= a_s$). Hence, we will approximate in Eq. (10) the point charge distribution for each step by a line of charge of constant density, $\eta_{AI} = +\frac{1}{4}/(1\times)$ for the AI step and $\eta_{AII} = -\frac{1}{4}/(1\times) = -\eta_{AI}$ for the AII step. Denoting by L_η the separation between the two charged lines, then

$$\Delta E_{Mad}(\sigma) \approx \frac{2(\eta_{AI})^2}{\epsilon}\log_e(L_\eta/L_{\eta,0}), \quad (11)$$

where the subscript 0 denotes the reference surface. Note that L_η is the *actual* spatial separation of the two charged lines whereas $L = 4a_sS$ is only an in-(001)plane measure of the separation between the AI and AII steps. For example, for a given S the AI + AII groove and the double A step would have the same L. On the other hand, L_η for the double A step is always larger than L_η for the AI + AII groove because the two charged lines in the double A step are not in the same (001) plane but are offset by two monolayers along the [001] direction (see Fig. 2a). For large S, however, the relative difference between L_η and L (defined as $(L_\eta - L)/L$) becomes negligibly small for both the AI + AII grooves and the double A steps. Hence, one can replace L_η in Eq. (11) by L. As results, the formation energies of both the AI + AII grooves and the double A steps diverge logarithmically with L (or equivalently with S).

(iii) *The relative stability between the AI + AII grooves and the double A steps:* As a result of a

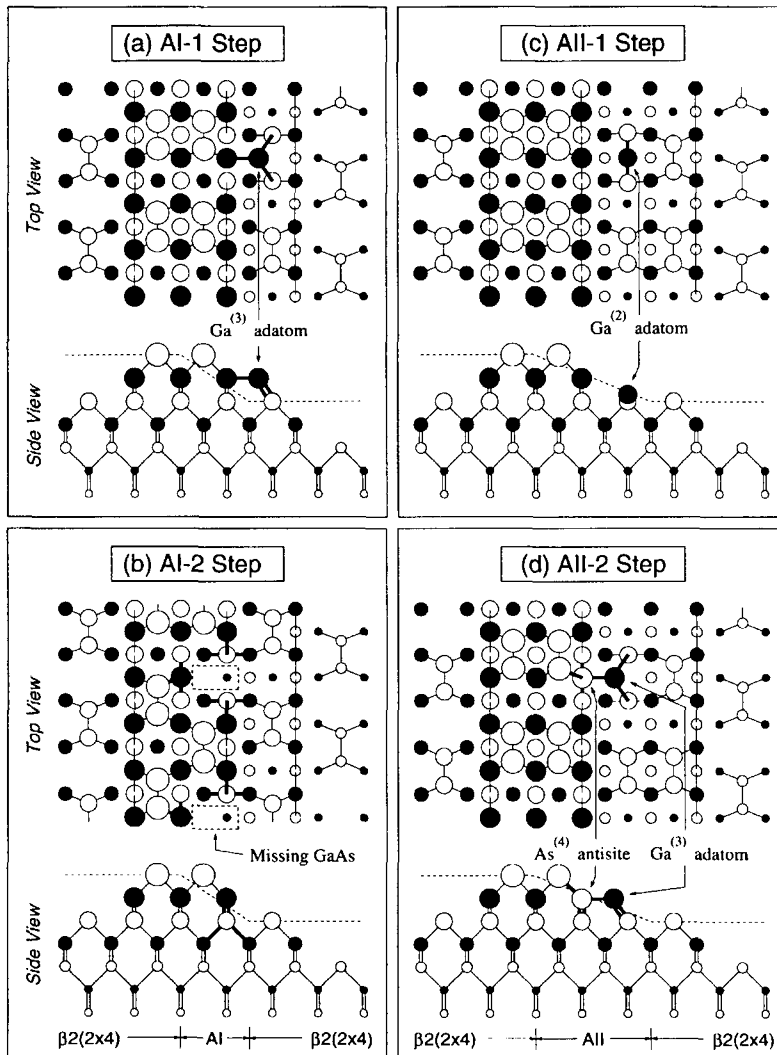

Fig. 5. Top and side views of the low energy bilayer A step models. The open and filled circles are As and Ga atoms, respectively, with decreasing sizes from surface into bulk. The bonds of surface adatoms, antisites and those atoms left by the surface vacancies are highlighted with thicker lines.

slightly larger L_η for the double A steps than L_η for the AI + AII grooves at a fixed S, the energy of an AI + AII groove is always slightly lower, although the difference approaches zero for large enough S, than that of the corresponding double A step.

3.2. Comparison with other A steps and grooves

To compare the formation energies of the AI + AII grooves and the double A steps with other competitive A grooves and A steps, we show in Fig. 5 several structural models for low energy single bilayer A steps. These step models are derived from charged primitive AI and AII steps with surface charge compensation. For a given primitive A step, say AI, there are a number of ways to achieve surface charge compensation. The resulting derivative steps are thus named here AI-n with $n = 1,2,3,\ldots$ etc. In contrast to the double A steps the derivative steps in Fig. 5 contain surface adatoms and native defects: The AI-1 step (4a) contains a threefold coordinated Ga adatom for every four step units ($4x$). The AI-2 step (4b) has a pair of surface Ga and As atoms missing for every $4a_s$. The AII-1 step (4c) contains a twofold coordinated Ga adatom per four step units whereas the AII-2 step in (4d) combines a surface As antisite with a threefold coordinated Ga adatom. As results, all three terms in Eq. (1), not just the Madelung term, enter the calculation of the formation energy. The construction and the calculation of the formation energies, although straightforward, involve lengthy discussions. The details are given elsewhere [16]. For simplicity, we have avoided using here the step orientation indices l and r of Section 1.

Fig. 6a compares as a function of the Ga chemical potential μ_{Ga} the formation energies of the $S = 0$ and $S = 1$ double bilayer height A steps with those of the single bilayer height A step models in Fig. 5. These energies have been normalized to per 1 × *and* per bilayer step height. In other words, the formation energies of the double A steps in Fig. 6a equal the usual steps formation energies per unit step divided by two. While the energies of the double A steps are independent of μ_{Ga}, the energies of the single bilayer A steps are in general a function of μ_{Ga}. A positive slope in Fig. 6a implies that the corresponding step structure is more As-rich than the underlying flat $\beta 2(2 \times 4)$ surface whereas a negative slope implies, instead, a more Ga-rich step. Excluding for a moment the "stoichiometric" $S = 0$ and $S = 1$ double A steps (heavy lines in Fig. 6), we see that the Ga-rich AI-1 step is stable for $-0.44 < \mu_{Ga} < -0.2$ eV, followed by the Ga-rich AI-2 step stable for $-0.65 < \mu_{Ga} < -0.44$ eV, and finally the As-rich AII-2 step is stable for $-0.7 < \mu_{Ga} < -0.65$ eV. The $S = 0$ double A step, on the other hand, is stable for $-0.7 < \mu_{Ga} < -0.29$ eV, thus excluding the AI-2 and AII-2 steps from our overall stability diagram. The chemical potential window for the $S = 0$ double A step covers a large portion of the Ga chemical potential range ($-0.7 < \mu_{Ga} < -0.2$ eV) over which the $\beta 2(2 \times 4)$ surface is stable (see Fig. 3). For $S \geq 1$, however, the single bilayer steps are more stable than the double A steps. Using the data presented in Fig. 6a, one can also show that the $S = 0$ double A step is stable with respect to any combination of the isolated, non-interacting (AI-n) + (AII-m) pairs, i.e., the (AI-1) + (AII-1), (AI-1) + (AII-2), (AI-2) + (AII-1) and (AI-2) + (AII-2) pairs.

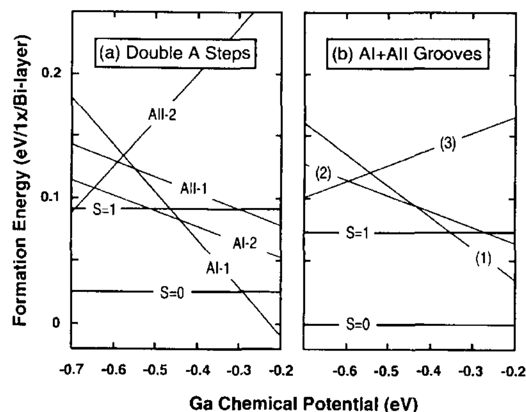

Fig. 6. Step formation energy versus Ga chemical potential for (a) the double A steps and (b) the AI + AII grooves. The reference energy is that of the flat $\beta 2(2 \times 4)$ surface. For comparison, the energies of the competing low energy A steps (of Fig. 5) and A grooves are also shown.

The formation energies of the AI + AII grooves are shown in Fig. 6b. The energies here are also normalized to eV per 1 × and per bilayer step height so that Fig. 6a and Fig. 6b can be compared directly. We compare the formation energies of the $S = 1$ AI + AII groove to three low energy (AI-n) + (AII-m) grooves made of the AI-n and AII-m derivative

steps in Fig. 5 where $m,n = 1,2$. We denote these grooves in Fig. 6b as: (1) Ga-rich (AI-1) + (AII-1), (2) Ga-rich (AI-2) + (AII-1) and (3) As-rich (AI-2) + (AII-2) grooves, respectively. Note that the $S = 0$ AI + AII groove is nothing but the flat $\beta 2(2 \times 4)$ surface. We see from Fig. 6b that the $S = 1$ AI + AII groove is stable for $-0.7 < \mu_{Ga} < -0.35$ eV, thus eliminating (2) and (3) from being stable A grooves. It is interesting to note in Fig. 6b that the remaining stable (1) (AI-1) + (AII-1) groove for $-0.35 < \mu_{Ga} < -0.2$ eV contains the AII-1 step segment which as a single A step is never stable (see Fig. 6a).

In view of the positive but low formation energies for the lowest energy $S = 0$ double A ($\Delta E = 0.025$ eV) and for the $S = 1$ AI + AII groove ($\Delta E = 0.074$ eV) with respect to the epitaxial growth temperature of typically 800 K (~ 0.075 eV), we expect that one should be able to identify experimentally such multiple step structures on GaAs(001) surfaces. It appears that previous STM work on GaAs(001) were largely focused on the stability of single bilayer height steps [10,11,17], although it has been reported that multi-bilayer height steps also exist during MOCVD growth [18,19]. This suggests the following possibilities: (i) Entropy effects could be important, i.e., the calculated $T = 0$ formation energy here does not include the configuration entropy which at elevated temperatures tends to favor single bilayer steps than multiple steps. (ii) The growth conditions used in experimental studies do not favor the formation of the multiple steps. (iii) Groove and double step structures were not carefully examined so far.

4. Summary

In this paper, we have examined two special types of step structures, the AI + AII grooves and the double A steps. They are special since the basic units of these step structures can be made by "cleaving" the underlying $\beta(2 \times 4)$ surface unit cell. No other surface modification such as atomic attachment (e.g., adatom) or detachment (e.g., vacancy formation) is involved. We demonstrated that these steps have potentially low formation energies since their formation from the $\beta 2(2 \times 4)$ surface involve no change in chemical species (reflected in the LCSM approach, $\Delta \omega_M = 0$ and $\Delta N_R = 0$). Our calculation showed indeed that both the $S = 1$ AI + AII groove and the $S = 0$ double A step are the most stable step configurations over a wide range of the Ga chemical potential.

Acknowledgements

This work was supported by the Advanced Energy Project, US Department of Energy, under contract No. DE-AC36-83CH10093 and by NREL Director's Development Fund.

References

[1] H.H. Farrell and C.J. Palmstrom, J. Vac. Sci. Technol. B 8 (1990) 903.
[2] E.J. Heller and M.G. Lagally, Appl. Phys. Lett. 60 (1992) 2675.
[3] H. Xu, T. Hashizume and T. Sakurai, Jpn. J. Appl. Phys. 32 (1993) 1511.
[4] V. Bressler-Hill, M. Wassermeier, K. Pond, R. Maboudian, G.A.D. Briggs, P.M. Petroff and W.H. Weinburg, J. Vac. Sci. Technol. B 10 (1992) 1881.
[5] Y. Haga, S. Miwa and E. Morita, J. Vac. Sci. Technol. B 12 (1994) 2107.
[6] T. Hashizume, Q.K. Xue, J. Zhou, A. Ichimiya and T. Sakurai, Phys. Rev. Lett. 73 (1994) 2208.
[7] J.E. Northrup and S. Froyen, Phys. Rev. B 50 (1994) 2015.
[8] D.J. Chadi, J. Vac. Sci. Technol. A 5 (1987) 834.
[9] T. Ide, A. Yamashita and T. Mizutani, Phys. Rev. B 46 (1992) 1905.
[10] E.J. Heller, Z.Y. Zhang and M.G. Lagally, Phys. Rev. Lett. 71 (1993) 743.
[11] M. Kasu, N. Kobayashi and H. Yamaguchi, Appl. Phys. Lett. 63 (1993) 678.
[12] S.B. Zhang and A. Zunger, Mater. Sci. Eng. B 30 (1995) 127.
[13] S.B. Zhang and A. Zunger, Phys. Rev. B 53 (1996) 1343.
[14] J.E. Northrup and S. Froyen, Phys. Rev. Lett. 71 (1993) 2276.
[15] S.B. Zhang and J.E. Northrup, Phys. Rev. Lett. 67 (1991) 2339; J.E. Northrup and S.B. Zhang, Phys. Rev. B 47 (1993) 6791; 50 (1994) 4962.
[16] S.B. Zhang and A. Zunger, unpublished.
[17] N. Ikarashi, T. Baba and K. Ishida, Appl. Phys. Lett. 62 (1993) 1632.
[18] M. Kasu and T. Fukui, Jpn. J. Appl. Phys. 31 (1992) L864.
[19] J. Ishizaki, S. Goto, M. Kishida, T. Fukui and H. Hasegawa, Jpn. J. Appl. Phys. 33 (1994) 721.